IMAGE PROCESSING OF COINCIDENT BINARY PATTERNS FROM GEOLOGICAL AND GEOPHYSICAL MAPS OF MINERALIZED AREAS

A.G. Fabbri*

Geological Survey of Canada

ABSTRACT

Binary images of different map units can be extracted, in registration with each other, from systematically digitized maps of the same area. The images are transformed and combined with one another to define regional geological situations which are described by the resulting new sets of coincident patterns.

Binary transformations provide quantitative measures of orientation and distributions of map units, and of interrelations between them. Fast parallel processing for producing the transformations can be obtained by compressing the binary data to one bit per pixel, and by using both Boolean and bit shift operators which are available on most computers.

To exemplify the approach, these techniques are used in the study by minicomputer of mineral resources - evaluations of two mineralized areas.

RÉSUMÉ

Les images binaires de diverses unités cartographiques peuvent être extraites, alignées les unes par rapport aux autres, à partir de cartes complètement numériques de la même zone. Ces images sont transformées et combinées les unes aux autres pour définir les situations géologiques régionales qui sont décrites par le nouveau groupe de diagrammes coïncidants obtenu.

Les transformations binaires donnent des mesures quantitatives de l'orientation et de la distribution des unités cartographiques et de l'interrelation entre elles. Le traitement parallèle rapide permettant de produire les transformations peut être obtenu en comprimant les données binaires à un bit par pixel et en utilisant les opérateurs de Boole et de décalage de bit qui sont accessibles sur tous les ordinateurs.

Afin de donner des exemples de ce genre d'approche, ces techniques sont utilisées dans l'étude par microordinateur des évaluations de ressources minérales de deux zones.

Introduction. One of the targets of image processing is the extraction of features from digital images. These are computer processable arrays of numbers in point-to-point correspondence with very small areas, pixels, in the original picture material. Image processing, in general, does not deal with hierarchically structured data, as is done in computer graphics. The reason is mostly one of computational convenience, but it is also because much pictorial data is currently available as raster formatted images, e. g., remotely sensed information, and this makes data integration easier.

Integrating geoscience data from different sources, offers the opportunity to use the computer for broadening the work of the economic geologist in the construction of maps which, in a quantitative form, represent the probability, associated with particular geological areas, of the occurrence of mineral deposits. Geometrical probability concepts have been developed for this purpose by Agterberg and Fabbri (1978) in the analysis of black and white images. In such binary images, each pixel indicates the presence of a given rock by the value binary 1, and its absence by a binary 0. Each rock type can be considered as a set of 1-valued pixels.

If a number of maps of ancillary data are also available, beside a geological map (e. g., mineral occurrence distribution maps, geophysical and geochemical contour maps, or remotely sensed pictures) it becomes feasible to develop statistical models for mineral resources estimation and to process images of maps as sets of pixels. The theory of sets can then be applied and processing is made easier. In general, such models are based on the relationships between known mineral occurrences and the characteristics of their neighborhoods in terms of the ancillary information.

Geometrical probability theory and applications have been developed in several fields indirectly related to geology, such as mathematical morphology (Matheron, 1975), geometrical probability and stereology (Serra, 1978) or mathematical geology (Switzer, 1976). Some of the applications have been performed on "image analysers": special purpose instruments in which a microprocessor, a television camera, and a microscope, or some other projecting devices, are interfaced (Hougardy, 1976).

Image analysers are real time hardware-built instruments which can become very powerful and complex systems if interfaced with large computers or if provided with sophisticated special purpose hardware, as the T.A.S. (Texture Analysing System) described by Nawrath and Serra (1979). Other applications are performed on even more powerful "pipeline processors" like the Cytocomputer, used by Gillies (1978) for real time pattern recognition. The cost of dedicated hardware, however, limits its availability, particularly in non-routine research work for which general purpose computers may be more accessible.

The approach pursued in this paper, is the analysis of relatively large images (1024 pixels x 1024 pixels) by a small general purpose computer. The images are digitized from geological maps and ancillary data related to uranium resources. The analysis has been and can be performed by one person, a geologist, who uses an interactive Fortran program package, GIAPP, developed by Fabbri (1980) for the analysis of geological data in picture form. In particular, GIAPP computes transformations of binary images which are in the compressed form of one bit per pixel.

Digitization of boundaries of geological maps. Geological maps contain lines depicting boundaries between different rock types and/or terrains of different ages. Within each bounded area, there occurs a different rock type or map unit. The units are classified using a legend in which colours and map units are associated. Graphical patterns and scattered symbols can also be substituted for colours when the latter are too expensive to reproduce. The colours on geological maps appear uniform to the human eye, but, unfortunately, are not so to automatic scanning devices (for example, uniform looking colours may consist of patterns of differently coloured dots). The maps also contain much additional information such as symbols for fractures, folds, mineral occurrences and various kinds of topographical features including geographical names. For these reasons, they may require redrafting (scribing) or recolouring in order to be efficiently scanned by automatic devices. It is also required that several maps of different types, but covering the same area on the ground, are digi-

tized so as to be in registration with each other.

Digitization by a 34 cm x 34 cm graphic tablet is here preferred as a practically simpler and faster means of producing raster binary images of map contours. Additional processing provides the automatic identification of all individual areas, and the interactive classification of the areas into map units. The extraction of binary images corresponding to each unit becomes a simple procedure.
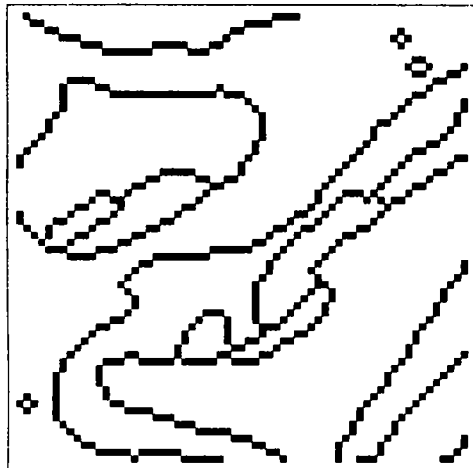

Figure 1a

Figure 1b

Figure 1: (a) magnified portion of edited binary image of geological boundaries digitized on the graphic tablet; (b) the image

in (a), after line thinning; and (c) the complete binary image (mosaic) of geological boundaries after preprocessing (image dimensions are 760 pixels x 1004 pixels; each pixel corresponds to a square area of side 167 m). Plots are obtained on a Versatec plotter.
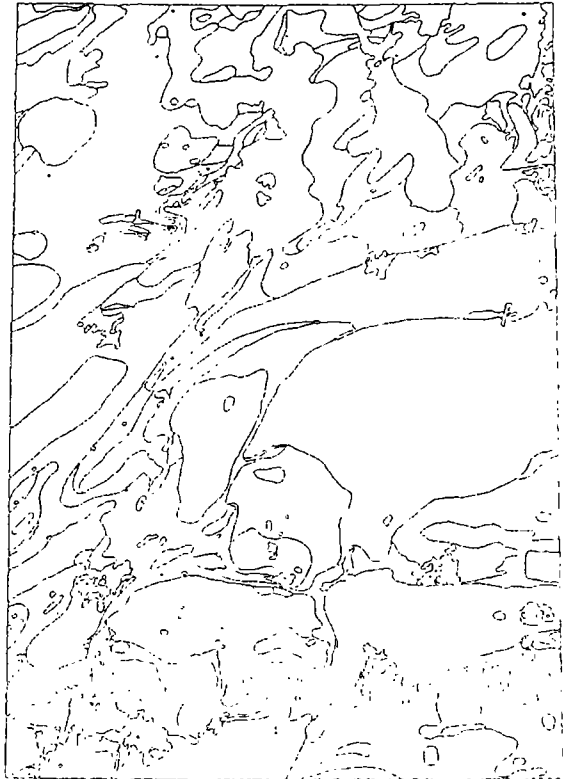

Figure 1c

Before digitizing, a number of corresponding rectangular subareas, smaller than the tablet size, are marked on all the maps of a set. Each subarea is placed on the tablet, and the digitization is performed by tracing all boundaries within the subarea with the stylus. Reference points and vectors obtained from the tablet are stored on magnetic tape for each subarea. They are later transformed into a raster image of boundaries by simply computing, for a given resolution, which squares in a superimposed regular grid, are crossed by the vectors. These squares become black pixels with value binary 1, as shown in Figure 1a. In cases of digitizing errors or of poor resolution, interactive editing is done while displaying magnified subareas of binary images on a

graphic screen. A line thinning algorithm is used to reduce the width of boundaries to a single pixel, as shown in Figure 1b. Several smaller images are then mapped into a larger one, like the image shown in Figure 1c, for a geological map. The image represents a 760 pixels x 1004 pixels mosaic of four subimages of 380 pixels x 502 pixels.

If the boundary lines are now described by connected chains of black pixels, it becomes a simple procedure to identify by unique numbers all areas enclosed within the boundaries (component labeling). The next processing step consists of displaying magnified subareas of the binary image of boundaries, and of interactively pointing once at the inside of each area to record a new map-unit label and its image coordinates. When this process is completed, a correspondence is established between the labels for the individual areas (components) and the new map-unit labels (phases). This correspondence is used for computing either a phase-labeled image (in which all pixels belonging to a same map unit are assigned its label (phase labeling)), or a different binary image for each map unit.

The desired information is captured from the geological map and the spatial correspondence with the original map is retained.

Quantification and identification of features from maps can also be achieved while remaining within the line graphics domain as, for example, was done by Bouille (1976). However, while some kinds of measurements, such as computing boundary lengths, are easier with graphic data than with raster data, it is not so easy to compute either logical operations between images or shrinking and expanding transformations on images. As described in the next section, operations and transformations, are intuitive and relatively simple with a raster data base.

In the remainder of this paper, descriptions are provided of what such computations can do in the field of regional resources assessment where, as a general case, it cannot be predicted in advance which kinds

of processing of the digitized data will be most useful.

Logical operations and transformations of binary compressed images.

If binary images are compressed to one bit per pixel, besides the obvious convenience in the reduction of storage space and in input/output time, logical operations between images and binary neighborhood transformations can be computed at relatively fast rates by combining Boolean and bit shift operators which exist on all general purpose computers. This is done in order to exploit the limited degree of parallellism permitted by the word length of the computer.

By these techniques, useful results are obtained in the analysis of binary images extracted from a boundary image, shown in Figure 1c, which represents the 1:250000 bedrock geology map of the Whiskey Jack Lake-Kasmere Lake area, in northwestern Manitoba where, during the past eight years, there has been exploration for uranium.

Binary neighborhood transformations are "erosions" and "dilatations" by structuring elements or templates. As described by Fabbri (1980), the latter can be imagined as small binary images which are swept across each pixel of an image in order to transform its 1 or 0 values into 0 or 1 according to the degree of coincidence between the pixels in its neighborhood and the corresponding pixels in the template. Figure 2 shows examples of logical operations and binary transformations for two images of the study area: the image of a map unit extracted from the image in Figure 1c, and the image of 10 km square cells centered around the locations of the 12 uranium occurrences known in the study area. By appropriate transformations, a variety of geometrical properties can be measured (often in terms of proportions of black to white pixels in the image before and after the transformations) which are immediately recomputed into geometrical probabilities.
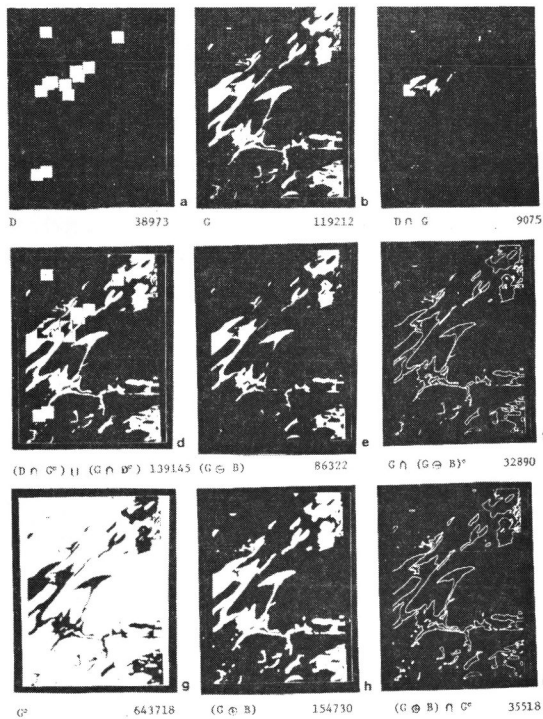
Figure 2: Transformations of binary images. The numbers of black pixels in the images (here displayed in white on a Tektronix 611 storage display unit) are shown below the right corners of the plots. Below the left corners the expressions for the transformations are shown. (a) image D of 61 pixels x 61 pixels neighborhoods (10 km x 10 km squares) of 12 uranium occurrences; (b) the image G of Aphebian pelitic metasediments; (c) the intersection (overlap or coincidence) between D and G; (d) the image produced by the .EXOR. or exclusive .OR.'ing logical operation (the union of two non-overlapping subsets) between D and G, which shows one image in the context of the other; (e) image G eroded by a 5 pixels x 5 pixels black template; (f) image of the pixels eroded from G; (g) the image of the complement or negation of G; (h) image G dilatated by a 5 pixels x 5 pixels black template; and (i) image of the black pixels "added" to the image G during the dilatation.

Extraction of patterns of areas related to uranium occurrences. If binary images are transformed and combined to obtain derived patterns as coincidencies of desirable characteristics, then the approach can represent a new geological tool in the study of regional resources. An application of this concept in the study area of northwestern Manitoba, is summarized in Figure 3. The application is described in more detail elsewhere by Fabbri and Kasvand (1981). In the study, four ancillary maps have been digitized: aeromagnetic anomaly contours, gravity anomaly contours, airborne gamma ray spectrometric contours of the ratio of equivalent uranium to equivalent thorium elemental concentrations, and the location of twelve 10 km square areas centered around each of the uranium occurrences known to exist in the area. By digitizing the geological and geophysical maps, images are extracted for several map units which are then related to each other according to the following model: (1) the gradational contact between Aphebian (Proterozoic) pelitic metasediments and Aphebian conglomeratic and psammitic metasediments, is a likely trap for uranium deposition; (2) aeromagnetic and gravity lows correspond to areas of thickest sedimentary piles; and (3) high values for the ratio of equivalent uranium / equivalent thorium, are related to the occurrence of granitic and pegmatitic intrusive rocks in which uranium concentration was locally observed. The coincidence of these factors should portray "environments" related to uranium mineralization within favourable structural and lithological settings.

A representation of this situation is modeled in Figure 3, where images are computed by combining one transformation by a structuring element, and several logical operations. Expressions for the operations and transformations can be written using the following symbols: B for a 5x5 black pixels structuring element set, $\oplus$ for dilatation of a set, $\cap$ for intersection, and $\cup$ for union of two sets. If mnemonics are used for indicating the binary images, we can write: G1 and G2 for the images of the two Aphebian metasedimentary units, AL for aeromagnetic anomaly lows, GL for gravity anomaly lows, and UT for the equivalent uranium / equivalent thorium ratios. Then the 850 m wide transitional-contact-zone binary image, set CT, between map units G1 and G2 can be written:

$$CT = (G1 \oplus B) \cap (G2 \oplus B).$$

The extracted pattern, shown in Figure 3d, can be written as:

$$EP = (AL \cap GL \cap CT) \cup (AL \cap UT \cap CT).$$

It is of interest to observe that, while CT represents 1.9% of the total image area, EP represents .5%. This can be expressed as a .005 probability that a random pixel sweeping throughout the image set EP, hits a black pixel. This probability can be appreciated by eye in Figure 3d, and it can be easily related to the context of other binary images. Representations of this kind are useful in the analysis of geological and ancillary data on resources.

This is a simple example of a technique for describing one particular uranium related "environment" by forcing geophysical anomaly contours into a discrete number of intervals. In general, it is the task of the specialist to design different models for deriving contour intervals for particular purposes. A specialist is also aware of the uncertainties associated with the data used for resources analysis: i. e., with the geological boundaries and the geophysical contours, or the unavoidable bias in a classification model based on the prior knowledge of one individual.

Measurements of orientation patterns of gravity anomaly contours. This second application is part of a preliminary geomathematical analysis made by Agterberg et al (1981), in the Southern District of Keewatin, Northwest Territories. The preferred orientation of the Bouguer anomalies in the area was investigated using digitized data similar to what has been described earlier. Figure 4a shows a binary image of the contours for 5 milligal intervals constructed for gravity measurements at intervals of about 12 km. The contours have been digitized from 1:500000 Bouguer anomaly gravity maps, where the anomaly reflects the specific gravity of rocks at deep levels below the surface. The preferred orientation of the gravity contours analysed is likely to represent the dominant structural trends of the rocks, in the upper part of

the Earth's crust, which may not be directly mappable on a geological map.

Clearly many contours in Figure 4a, have a prominent northeast-southwest trend, whereas other contours have a weaker orientation perpendicular to this direction. A simple way to study the orientation of the contours in a given area is to compute a rose diagram. This is obtained by approximating the contours by successive straight line segments that are sufficiently short, and by constructing the histogram of the combined lengths of all line-segments pointing in directions bounded by class limits (e. g., 10 degrees apart). RODIA (for ROse DIAgram) is an algorithm written by Agterberg (1979) which was used for constructing a smoothed histogram of the contact between black and white pixels in a binary image.

Several experiments have been performed on the image (of size 915 pixels x 915 pixels) of all gravity anomaly contours shown in Figure 4a. Each pixel corresponds to a square area of side 500 m. First, the image of contours was changed into another image, the "zebra map" shown in Figure 4c, by extracting the binary images of every other interval and computing their union. One interval is shown in Figure 4b, between values of -60 and -65 milligals. Next a square subarea of 768 pixels x 768 pixels was outlined on the zebra map, so that it is at least 5 pixels removed from the edges of the zebra map in the east-west and north-south directions. The square was divided into subareas according to two different methods. A first set of three subareas B, A, and C, shown in Figures 4e and 4f, respectively, was obtained by intersecting the zebra map with binary images (masks) like the one shown in Figure 4d. Area A in Figure 4f is roughly triangular in shape and covers the northwestern part of the region; area B, in Figure 4e, is a southwest-northeast oriented strip across the center; and area C, in Figure 4f, covers the southeastern part of the region. A second set of subareas was obtained simply by dividing the 768 pixels x 768 pixels binary image of the zebra map, into 9 equal-area images of 256 pixels x 256 pixels. These areas have been numbered from 1 to 9, from top to bottom and from left to right: they are shown as mosaics of plots in Figures 4g and 4h.
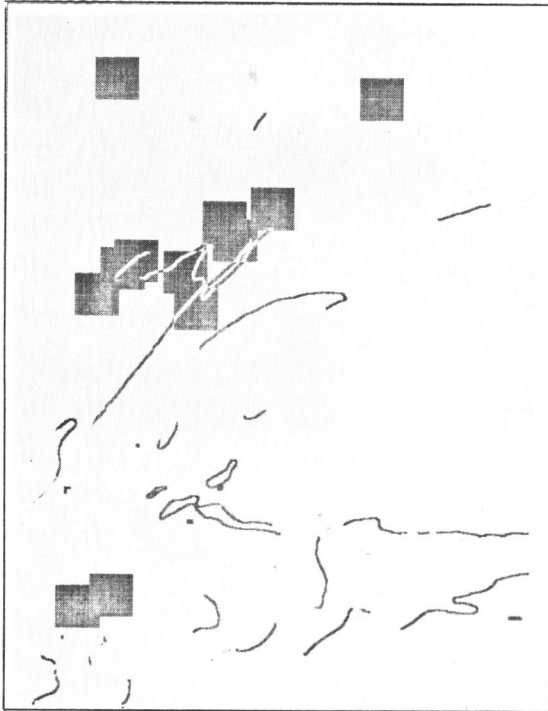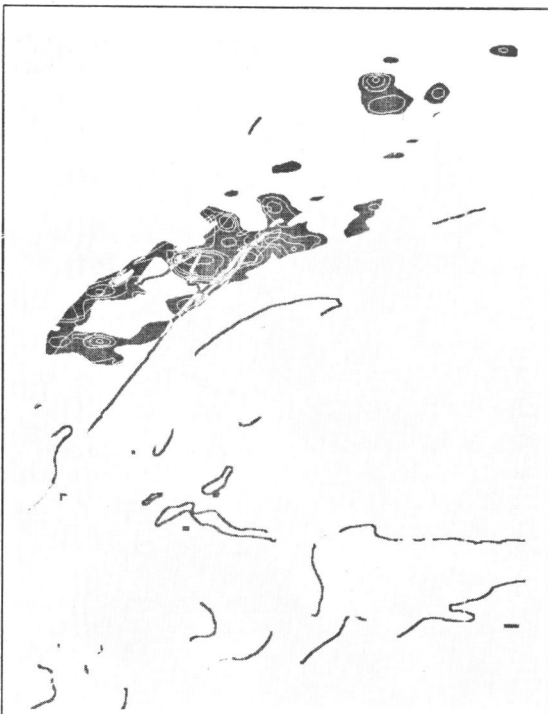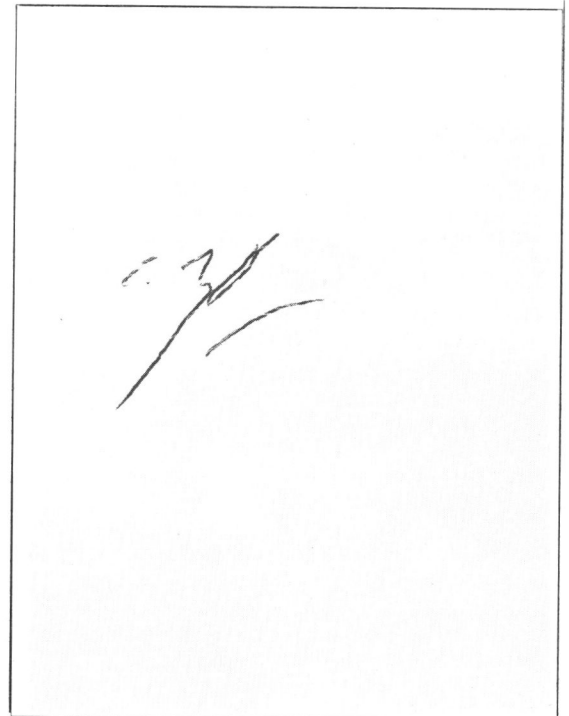
Figure 3a

Figure 3b

Figure 3c

Figure 3d

geological boundary map of the area in Figure 41.

Figure 3: Extraction of pattern of coincidencies. (a)intersection of the two dilatated binary images of Aphebian (Proterozoic) pelitic metasediments, and Aphebian conglomeratic and psammitic metasediments. The image shows the set CT, of the 850 m wide zones of contact between the two geological map units. The set CT is exclusive OR'ed with the image D, of 61 x 61 black pixels squares centered around 12 uranium occurrence pixels. (b) intersection of the images of aeromagnetic anomaly lows, AL (less than 2100 gammas) and of gravity lows , GL (less than -70 milligals) exclusive OR'ed with CT. (c) intersection of the image AL with the image of equivalent uranium / equivalent thorium ratio highs, UT (greater than .2), exclusive OR'ed with CT. (d) partitioning of CT into likely sites for new discoveries: i. e., the extracted pattern EP. Additional explanation is in the text.

Each of the 12 binary images was shifted across the image of the zebra map, for distances of 0 to 5 pixels in eastern, southern, and western directions. The geometrical covariance, i. e., the number of coinciding black pixels in the two images was measured for each shift using GIAPP. The result was a set of 61 covariance values which were used as the input to RODIA. Such an input for subarea 3 of figure 4g, is shown in Table I. From this array a rose diagram is computed. The results should be evaluated by comparing histograms for different subareas with one another.

In Figure 5, the histograms are shown for subareas A, B, and C. In each histogram, the frequencies are plotted vertically, and the corresponding directions are plotted for clockwise rotation in the horizontal direction starting from 0 degrees for the west-to-east direction, and ending with 180 degrees for the east-to-west direction. These patterns of histograms show that there are two main preferred orientations in areas A, B, and C, with the northeast orientation better developed than the northwest orientation in all three subareas. The strongly preferred orientation in area B (Figure 4e) is reflected in the pronounced northeast trend of the surface rocks as shown on the

In Figure 6, the histograms are shown for subareas 1 to 9 of Figures 4g and 4h, in their respective locations. Most of these patterns of orientations confirm the results obtained for areas A, B, and C; however, locally one or both of the preferred orientations may be less well developed than in other parts of the study region. The northwest orientation, well developed in areas 4 and 6 of Figure 4h, is possibly related to younger, high level granite masses, in area 6, and to abundant high level granite plutons in area 4. According to K. E. Eade (Geological Survey of Canada, personal communication) the northwest orientation represents a younger trend in the crust associated with granitic plutons. Such trend, not well expressed in the orientation of the geological boundaries, is of interest for the interpretation of the economic geology of the region.

Concluding remarks. In this paper, two experiments on large binary images have been described for the extraction of patterns of coincidencies and of orientations of features from regional geological and geophysical maps in areas in northern Canada, which are being assessed for uranium resources.

The approach consists of using Fortran programming on a general purpose small computer (a Modcomp II with 64 K words of 16 bits read/write memory), digitizing boundaries from maps in registration, and of computing special transformations of binary compressed images extracted from the digitized boundaries. The philosophy of the technique is to enable one single geologist to control applications to mineral resources.

An additional advantage of the approach, is that statistical concepts of geometrical probabilities are observable as sets of binary images. This facilitates both interpretation and communication.

References.

Agterberg, F. P., 1979, Algorithm to estimate the frequency values of rose diagrams for boundaries of map features: Computers & Geosciences, v. 5, p. 215-230.

Agterberg, F. P., Chung, C. F., Divi, S. R., Eade, K. E., and Fabbri, A. G., 1981, Preliminary geomathematical analysis of geological, mineral occurrence, and geophysical data, Southern District of Keewatin, Northwest Territories: Geol. Surv. Canada, Open File 718 (in press).

Agterberg, F. P., and Fabbri, A. G., 1978a, Spatial correlation of stratigraphic units quantified from geological maps: Computers and Geosciences, v. 4, p. 285-294.

Bouille, F., 1976, Graph theory and digitization of geological maps: Jour. Int. Assoc. Math. Geol., v. 8, p. 375-393.

Fabbri, A. G., 1980, GIAPP: geological image analysis program package for estimating geometrical probabilities: Computers and Geosciences, v. 6, p. 153-161.

Fabbri, A. G., and Kasvand, T., 1981, Applications at the interface between pattern recognition and geology: Sciences de la Terre (in press).

Gillies, A. W., 1978, An image processing computer which learns by example: in Nevatia, R., Ed., Image understanding systems and industrial applications: Proc. of the Soc. of Photo-Optical Instrumentation Engineers, SPPIE, Aug. 30-31, 1978, Sandiego, California, v. 155, p. 120-126.

Hougardy, H. P., 1975, Automatic image analysing instruments today: Proc. 4th Int. Cong. for Stereology, Gaithersburg, Maryland, NBS Special Publication 431, p. 141-148.

Matheron, G., 1975, Random sets and integral geometry: John Wiley & Sons, New York, 261 p.

Nawrath, R., and Serra, J, 1979, Quantitative image analysis: Theory and instrumentation: Microscopica Acta, v. 82, p. 101-111.

Switzer, P., 1976, Applications of random process models to the description of spatial distributions of qualitative geologic variables: in Merriam, D. F., Ed., Random processes in geology: New York, Springer-Verlag, p. 124-134.

Serra, J., 1978, One, two, three,... infinity: in Miles, R. L., and Serra, J., Eds., Geometrical probability and biological structure: Buffon's 200th anniversary: New York, Springer-Verlag, 338 p., p. 137-152.

Figure 4: Processing for orientation patterns. (a) binary image of thinned gravity contours (of dimension 915 pixels x 915 pixels; each pixel corresponds to a square area of side 500 m); (b) extraction of image of gravity anomaly interval -60/-65 milligals; (c) extraction of "zebra map", the union of images for every other interval extracted from (a); (d) a binary image mask, for partitioning (c); (e) intersection between (c) and (d) to produce image of subarea B; (f) subareas A (upper left) and C (lower right) extracted from (c) by two masks complementary to (d) within a 768 pixels x 768 pixels square; (g) 256 pixels x 256 pixels subareas 1,3,5,7, and 9 extracted from (c); (h) 256 pixels x 256 pixels subareas 2,4,6, and 8 extracted from (c); and (i) binary image of thinned geological boundaries digitized in registration with (a).
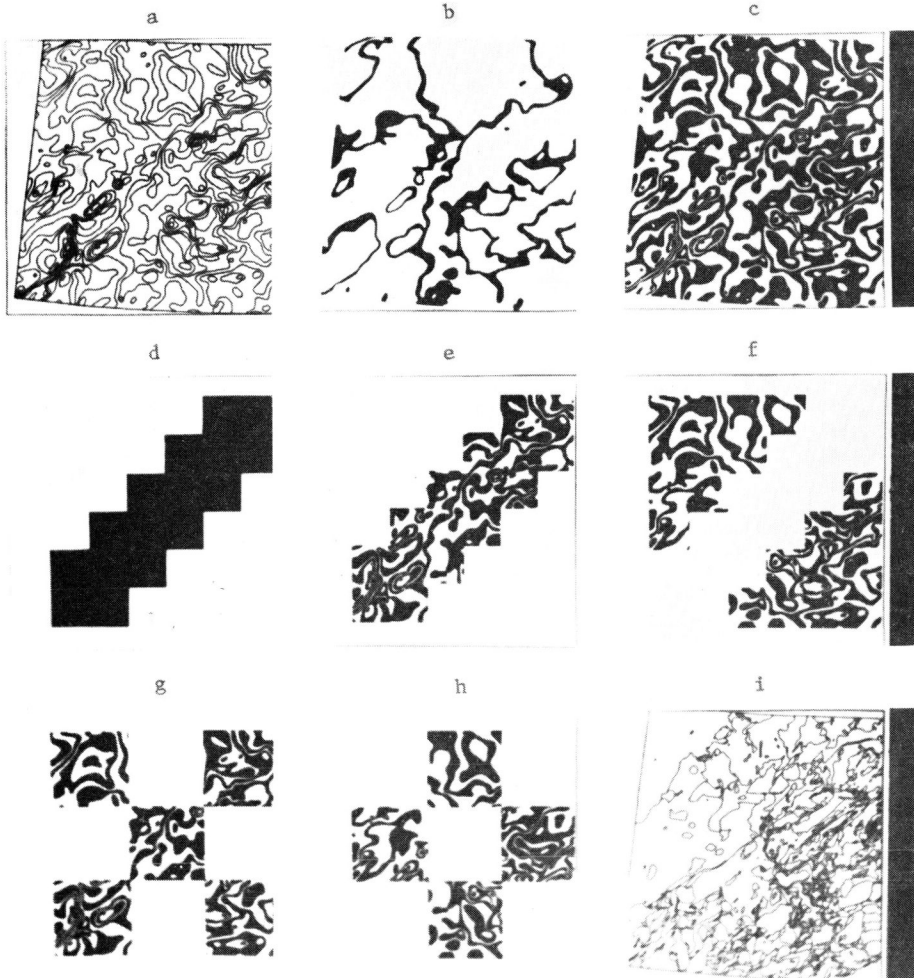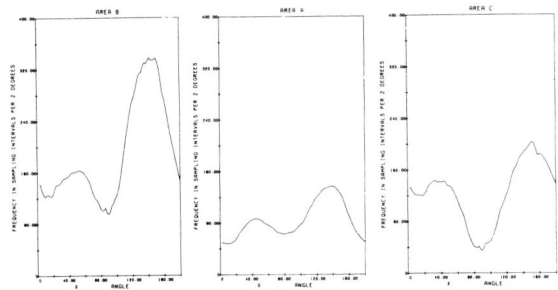
Figure 4

Figure 5: The rose diagrams computed for subareas A, B, and C of Figures 4e and 4f.
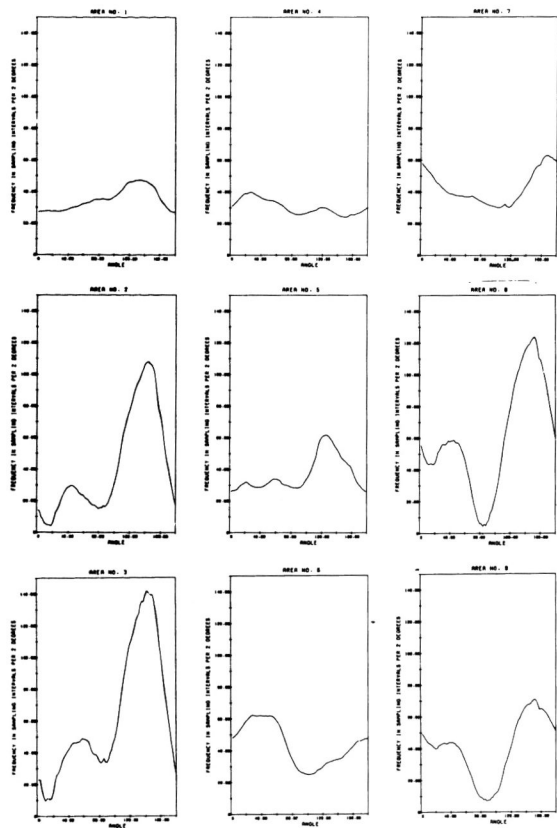
Figure 6: The rose diagrams computed for subareas 1 to 9 of Figures 4g and 4h.

Table 1: Geometrical covariance array for computing the rose diagram plot shown in Figure 6 for subarea 3 of Figure 4g. Coordinate values and signs indicate image shifts in pixels for west (−), east (+) and south (−) directions. Numbers of coincident black pixels are shown.

	-5	-4	-3	-2	-1	0	1	2	3	4	5
0	22667.	24107.	25740.	27483.	29273.	31078.	29227.	27390.	25599.	23919.	22433.
-1	23332.	24784.	26381.	27961.	29223.	29279.	28012.	26331.	24636.	23051.	21706.
-2	23750.	25074.	26368.	27418.	27813.	27489.	26431.	25049.	23533.	22160.	21031.
-3	23798.	24812.	25690.	26173.	26195.	25756.	24852.	23684.	22467.	21348.	20429.
-4	23445.	24142.	24592.	24746.	24597.	24152.	23373.	22447.	21503.	20665.	19926.
-5	22836.	23208.	23402.	23384.	23180.	22741.	22100.	21423.	20758.	20097.	19493.
	-5	-4	-3	-2	-1	0	1	2	3	4	5